Efficiency enhancement in two-cell CIGS photovoltaic system with low-cost optical spectral splitter

Carlo Maragliano,[1,*] Harry Apostoleris,[1] Matteo Bronzoni,[2] Stefano Rampino,[2] Marco Stefancich,[2] and Matteo Chiesa[1]

[1]*Laboratory for Energy and NanoScience (LENS), Center for Future Energy Systems (iFES), Masdar Institute of Science and Technology, P.O. Box 54224, Abu Dhabi, United Arab Emirates*

[2]*Istituto Materiali per l'Elettronica ed il Magnetismo, Consiglio Nazionale delle Ricerche, Parco Area delle Scienze 37/A - 43124 Parma, Italy*

**cmaragliano@masdar.ac.ae*

Abstract: Spectrum splitting represents a valid alternative to multi-junction solar cells for broadband light-to-electricity conversion. While this concept has existed for decades, its adoption at the industrial scale is still stifled by high manufacturing costs and inability to scale to large areas. Here we report the experimental validation of a novel design that could allow the widespread adoption of spectrum splitting as a low-cost approach to high efficiency photovoltaic conversion. Our system consists of a prismatic lens that can be manufactured using the same methods employed for conventional CPV optic production, and two inexpensive $CuInGaSe_2$ (CIGS) solar cells having different composition and, thus, band gaps. We demonstrate a large improvement in cell efficiency under the splitter and show how this can lead to substantial increases in system output at competitive cost using existing technologies.

OCIS codes: (040.5350) Photovoltaic; (120.5710) Refraction.

References and links

1. A. Imenes and D. Mills, "Spectral beam splitting technology for increased conversion efficiency in solar concentrating systems: a review," Sol. Energy Mater. Sol. Cells **84**(1-4), 19–69 (2004).
2. A. Mojiri, R. Taylor, E. Thomsen, and G. Rosengarten, "Spectral beam splitting for efficient conversion of solar energy—A review," Renew. Sustain. Energy Rev. **28**, 654–663 (2013).
3. H. Cotal, C. Fetzer, J. Boisvert, G. Kinsey, R. King, P. Hebert, H. Yoon, and N. Karam, "III–V multijunction solar cells for concentrating photovoltaics," Energy Environ. Sci. **2**(2), 174–192 (2009).
4. M. A. Green, M. J. Keevers, I. Thomas, J. B. Lasich, K. Emery, and R. R. King, "40% efficient sunlight to electricity conversion," Prog. Photovolt. Res. Appl. **23**(6), 685–691 (2015).
5. J. D. McCambridge, M. A. Steiner, B. L. Unger, K. A. Emery, E. L. Christensen, M. W. Wanlass, A. L. Gray, L. Takacs, R. Buelow, T. A. McCollum, J. W. Ashmead, G. R. Schmidt, A. W. Haas, J. R. Wilcox, J. Van Meter, J. L. Gray, D. T. Moore, A. M. Barnett, and R. J. Schwartz, "Compact spectrum splitting photovoltaic module with high efficiency," Prog. Photovolt. Res. Appl. **19**(3), 352–360 (2011).
6. B. Mitchell, G. Peharz, G. Siefer, M. Peters, T. Gandy, J. C. Goldschmidt, J. Benick, S. W. Glunz, A. W. Bett, and F. Dimroth, "Four-junction spectral beam-splitting photovoltaic receiver with high optical efficiency," Prog. Photovolt. Res. Appl. **19**(1), 61–72 (2011).
7. R. K. Kostuk, J. Castillo, J. M. Russo, and G. Rosenberg, "Spectral-shifting and holographic planar concentrators for use with photovoltaic solar cells," Proc. SPIE **6649**, 66490I (2007).
8. D. Zhang, M. Gordon, J. M. Russo, S. Vorndran, M. Escarra, H. Atwater, and R. K. Kostuk, "Reflection hologram solar spectrum-splitting filters," Proc. SPIE **8469**, 846807 (2012).
9. M. D. Escarra, S. Darbe, E. C. Warmann, and H. Atwater, "Spectrum-splitting photovoltaics: Holographic spectrum splitting in eight-junction, ultra-high efficiency module," in IEEE 39th Photovoltaic Specialists Conference (PVSC) (2013), pp. 1852–1855.
10. G. Kim, J. A. Dominguez-Caballero, H. Lee, D. J. Friedman, and R. Menon, "Increased photovoltaic power output via diffractive spectrum separation," Phys. Rev. Lett. **110**(12), 123901 (2013).

#252378 Received 21 Oct 2015; revised 26 Nov 2015; accepted 27 Nov 2015; published 14 Dec 2015

11. P. Wang, J. A. Dominguez-Caballero, D. J. Friedman, and R. Menon, "A new class of multi-bandgap high-efficiency photovoltaics enabled by broadband diffractive optics," Prog. Photovolt. Res. Appl. (2014), http://onlinelibrary.wiley.com/doi/10.1002/pip.2516/full.
12. C. Maragliano, M. Chiesa, and M. Stefancich, "Point-focus spectral splitting solar concentrator for multiple cells concentrating photovoltaic system," J. Opt. **17**(10), 105901 (2015).
13. D. C. Miller and S. R. Kurtz, "Durability of Fresnel lenses: a review specific to the concentrating photovoltaic application," Sol. Energy Mater. Sol. Cells **95**(8), 2037–2068 (2011).
14. http://pvinsights.com/index.php
15. H. Luque, *Handbook of Photovoltaic Science and Engineering* (John Wiley & Sons, 2003)
16. M. Contreras, L. M. Mansfield, B. Egaas, J. Li, M. Romero, R. Noufi, E. Rudiger-Voigt, and W. Mannstadt, "Improved energy conversion efficiency in wide bandgap Cu (In, Ga) Se 2 solar cells," in 37th IEEE Photovoltaic Specialists Conference (PVSC) (2011), pp. 000026–000031.
17. S. Ishizuka, A. Yamada, P. J. Fons, H. Shibata, and S. Niki, "Structural tuning of wide-gap chalcopyrite CuGaSe2 thin films and highly efficient solar cells: differences from narrow-gap Cu(In,Ga)Se2," Prog. Photovolt. Res. Appl. **22**, 821–829 (2014).
18. M. Steichen, M. Thomassey, S. Siebentritt, and P. J. Dale, "Controlled electrodeposition of Cu-Ga from a deep eutectic solvent for low cost fabrication of CuGaSe2 thin film solar cells," Phys. Chem. Chem. Phys. **13**(10), 4292–4302 (2011).
19. R. Herberholz, V. Nadenau, U. Rühle, C. Köble, H. Schock, and B. Dimmler, "Prospects of wide-gap chalcopyrites for thin film photovoltaic modules," Sol. Energy Mater. Sol. Cells **49**(1-4), 227–237 (1997).
20. S. Rampino, N. Armani, F. Bissoli, M. Bronzoni, D. Calestani, M. Calicchio, N. Delmonte, E. Gilioli, E. Gombia, R. Mosca, L. Nasi, F. Pattini, A. Zappettini, and M. Mazzer, "15% efficient Cu(In,Ga)Se_2 solar cells obtained by low-temperature pulsed electron deposition," Appl. Phys. Lett. **101**(13), 132107 (2012).
21. S. Rampino, M. Bronzoni, L. Colace, P. Frigeri, E. Gombia, C. Maragliano, F. Mezzadri, L. Nasi, L. Seravalli, F. Pattini, G. Trevisi, M. Motapothula, T. Venkatesan, and E. Gilioli, "Low-temperature growth of single-crystal Cu(In,Ga)Se2 films by pulsed electron deposition technique," Sol. Energy Mater. Sol. Cells **133**, 82–86 (2015).
22. J. M. Russo, D. Zhang, M. Gordon, S. Vorndran, Y. Wu, and R. K. Kostuk, "Spectrum splitting metrics and effect of filter characteristics on photovoltaic system performance," Opt. Express **22**(S2 Suppl 2), A528–A541 (2014).
23. H. Baig, K. C. Heasman, and T. K. Mallick, "Non-uniform illumination in concentrating solar cells," Renew. Sustain. Energy Rev. **16**(8), 5890–5909 (2012).
24. A. W. Horowitz, M. Woodhouse, G. Smestad, and H. Lee, A Bottom-up Cost Analysis of a High Concentration PV Module, in Proceedings of the 11th International Conference on Concentrator Photovoltaic Systems, CPV-11 (AIP, 2015), Vol. 1679, p. 100001
25. D. Feldman, "Photovoltaic (PV) pricing trends: historical, recent, and near-term projections," Technical Report, USDOE Office of Energy Efficiency and Renewable Energy Solar Energy Technologies Program (2014).
26. M. A. Green, K. Emery, Y. Hishikawa, W. Warta, and E. D. Dunlop, "Solar cell efficiency tables (Version 45)," Prog. Photovolt. Res. Appl. **23**(1), 1–9 (2015).
27. P. Benítez, J. C. Miñano, P. Zamora, R. Mohedano, A. Cvetkovic, M. Buljan, J. Chaves, and M. Hernández, "High performance Fresnel-based photovoltaic concentrator," Opt. Express **18**(S1), A25–A40 (2010).
28. R. Margolis, C. Coggeshall, and J. Zuboy, "SunShot vision study," US Dept. of Energy, (2012).

1. Introduction

Spectrum splitting has regained attention in recent years as an alternative pathway to high-efficiency solar energy conversion [1,2]. In contrast to multi-junction (MJ) solar cells, in which expensive lattice-matched materials with different band gaps are stacked in series to allow for spontaneous light filtration [3], spectral splitting uses an optical element designed to separate the sunlight into laterally spaced wavelength bands, which are then directed to band-matched absorbers. The main advantage of this solution is to eliminate the lattice-matching requirement of MJ cells, allowing a wider range of materials and more economical fabrication methods to be used. In this way, spectral splitting systems may achieve substantial cost savings relative to MJ-based systems, even at much lower concentrations, leading additionally to more relaxed sun-tracking requirements and thereby further reductions in cost. In addition spectrum splitting allows more flexibility in the electrical wiring of the system, enabling easier satisfaction of current-matching requirements for series connections by varying cell size, or alternative series/parallel connections. This in turn allows spectrum splitting systems to achieve higher theoretical efficiencies than MJ cells [1].

Spectrum splitting using dichroic filters [4,5], beam splitters [6], holographic [7–9] and diffractive elements [10,11] has been demonstrated. The main disadvantages of these optical designs are the high cost of materials and/or manufacturing processes, low optical efficiency

#252378 Received 21 Oct 2015; revised 26 Nov 2015; accepted 27 Nov 2015; published 14 Dec 2015

and inability to scale to industrial production. These aspects, together with the high complexity of the systems, have stalled spectrum-splitting technology in the early development stage.

Here we describe and experimentally validate a low cost spectral splitter suitable for industrial mass production. The optical element is a Fresnel-like prismatic lens made of inexpensive plastic and fabricated by injection molding, the same technique used for industrial scale lenses [12]. The principle of operation of the device is discussed and we evaluate its performance under real sunlight conditions when coupled with a pair of inexpensive thin film $CuInGaSe_2$ (CIGS) solar cells of different band gaps. Finally, the cost-competitiveness of the system is analysed against other PV technologies. Given the low cost of the optical device, and by choosing economical power converting cells, we project that a system based on our device could provide a cost-competitive energy generation solution ready for industrial scaling, with the potential to displace MJ solar cell technologies and to reduce the price-gap with crystalline silicon PV modules.

2. Results and discussions

2.1 Spectral splitter concentrator

The optical element is designed to simultaneously split and concentrate sunlight. Figure 1(a) shows a schematic of the splitting of a white beam by a dispersive prism, the fundamental building block of our design. The separation among distinct wavelengths observed at the receiver plane depends both on the geometry of the prism and the construction material. Given the angle formed by the normal to the entrance facet and the light rays I_1 and the apical angle of the prism *A*, the y position y_λ of a given wavelength on the receiver, taking the height of the incident light on the prism as reference, is:

$$y_\lambda = Z \cdot \tan\left(D_\lambda\right) \tag{1}$$

where *Z* is the distance between the prism and the receiver and D_λ is the deviation angle between the incoming and outgoing ray, given by:

$$D_\lambda = I_1 - A + \sin^{-1}\left\{ n_\lambda \cdot \sin\left[A - \sin^{-1}\left(\frac{1}{n_\lambda} \cdot \sin\left(I_1\right) \right) \right] \right\} \tag{2}$$

with n_λ being the refractive index of the material. As n_λ depends on the wavelength according to material dispersion, different colors are separated in space at the receiver surface. Thereby a single prism acts by itself as a spectral splitter as is seen by the conversion of white light into a 'rainbow' when passed through it. To achieve concentration, we combine several prisms oriented so that the rainbow projections of all of the prisms overlap. This concept is illustrated in Fig. 1(b) where the y-z section of the optical element is shown. As it can be observed, the y-z section consists of a set of prisms arranged along a curved line so that the light rays of a given wavelength converge at the same height on the receiver. This design enables concentration along the y direction since the number of rays converging at the receiver increases linearly with the number of prisms without affecting the light splitting. To allow for additional concentration in the x direction, each prism was divided into an odd number of sections, as illustrated in Fig. 1(c), and their exit facets were tilted by a small angle u around the y-axis to superimpose the images of each section. The angle u for each section was chosen to preserve continuity of the element surface and was kept small to minimize color splitting along the x direction. By tilting the prismatic segments to achieve x-concentration, spectrally dispersed light hits the receiver at an angle. This generates a concentration gradient along the

#252378 Received 21 Oct 2015; revised 26 Nov 2015; accepted 27 Nov 2015; published 14 Dec 2015

x-axis, as dispersed light is more concentrated at the center of the pattern than at its extremes. As a consequence, the light projected by the splitter shows reduced spectral separation at the extreme x positions of the receiver plane. To compensate for this effect, the angle u was optimized for each section in such a way that central sections would concentrate less than external ones. Figure 1(d) shows a schematic of the final design, which has an approximate area of 7x3 cm^2, where 30 prisms are arranged. As our construction material, we use polycarbonate (PC), a thermoplastic with high transmissivity and distinctive dispersion characteristics [12]. While PC can suffer from UV degradation when exposed to sunlight for long period of times, this can be prevented by using additives or by overlying the splitter with glass [13]. Figure 1(e) shows the calculated y position of each wavelength of the solar spectrum on the receiver, where the height of the lowest wavelength of the visible range (380 nm) is taken as reference. The separation between wavelengths is not linear and follows the dispersion curve of PC: for an incidence angle I_1 of 10 degrees, the spectrum (here represented from 380 to 1800 nm) is spread over approximately 4.5 cm, with most of the range occupied by visible light (380 to 740 nm). When the splitter is illuminated with perfectly collimated light, the minimum width of a single wavelength component projected on the receiver along the y-direction is given by the width of each prismatic segment. When, on the other hand, light with a finite divergence angle (i.e. sunlight) is used, this width is increased, causing some overlap between different colors. The concentration ratio is also wavelength dependent as displayed in Fig. 1(f), increasing up to around 210x under sunlight illumination in the infrared region above 1500 nm. The comparison between the solar spectrum and the concentration factor curve in Fig. 1(f) shows that the device reaches higher concentrations for the infrared region, which is the part of the solar spectrum that has the lower intensity. This creates a more uniform illumination of the surface than would a linear mapping of wavelength to position, as shown in Fig. 1(g). The curve, obtained by combining Figs. 1(e) and (f), displays the spatial dependence of the total light intensity, normalized to the full spectrum direct solar irradiance striking the surface of the splitter (here 1 sun = 1000 W/m^2). It confirms the spectral separation and shows that flux intensities as high as 2.5 suns are achieved in the visible range and intensities above 1 sun are still obtained in the near infrared region.

#252378 Received 21 Oct 2015; revised 26 Nov 2015; accepted 27 Nov 2015; published 14 Dec 2015

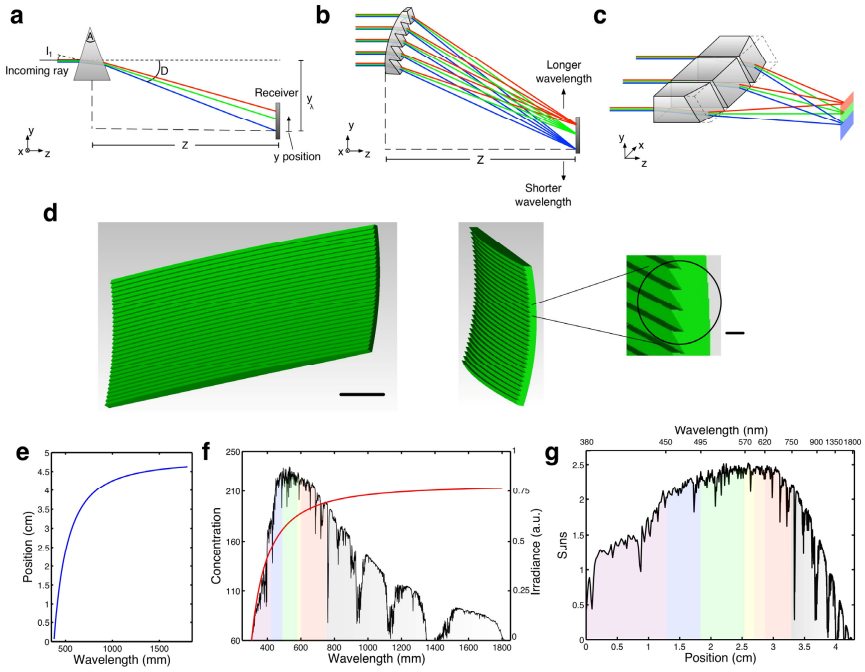

Fig. 1. (a) Splitting by a single prism. The white beam is broken up into its constituent spectral colors, which are separated at the receiver plane. (b) Schematic of the y-z section of the spectral splitter concentrator. A set of prisms is arranged on a curved line to allow for light concentration while maintaining the color splitting. (c) Conceptual drawing of a single prism. Each prism is divided into an odd number of sections, the exit facets of which are tilted of a small angle around the y axis to superimpose the section-generated image on the one of the central portion. (d) Final design of the spectral splitter concentrator. The approximate area is 7x3 cm^2, with an average thickness of ~ 2 mm. The magnification on the right of the figure shows the shape of a single prism. Markers (from left to right): 1 cm and 2 mm. (e) Calculation of the position of each wavelength on the receiver, referenced with respect to the lowest wavelength of the visible range (380 nm). A dispersion of the solar spectrum (380-1800 nm) over approximately 4.5 cm is showed, with most of the range occupied by visible light. (f) Calculated concentration factor for each wavelength of the spectral splitter concentrator. The curve follows the same trend of the spatial displacement: the device concentrates more the part of the spectrum that has the lower intensity. (g) Calculated concentration magnification ratio, normalized with respect to direct full spectrum (AM1.5D), plotted versus position on the receiver and versus wavelength. Values as high as 2.5 suns are obtained across the visible range, while factors in between 2 and 0.5 suns are predicted in the infrared range below 1350 nm.

The device, pictured in Fig. 2(a), was fabricated by injection molding, a technique widely used for commercial lenses that allows for low-cost, large-scale replication. In order to verify the fabrication process, the prototype was experimentally characterized and results were compared with simulations obtained by importing the model of the device into a commercial ray-tracing tool. Figure 2(b) shows a simulated two-dimensional map of the light intensity at the receiver surface for different wavelengths (480, 532, 650, 1000 and 1500 nm) together with a picture of the experimental light pattern obtained under solar light illumination. To validate our results we carried out a power and spectral analysis with moving probes feeding respectively to a power meter (Newport 1918-C) and a spectrometer (Ocean Optics USB4000-UV-VIS). Figure 2(c) plots the light intensity measured over the length of the projected pattern. We note that the curve follows the same trend predicted in Fig. 1(g), with a maximum intensity of 2 ± 0.1 suns achieved across the red-orange region. By comparing the experimental light profile with that computed with the analytical model, we obtain an average optical efficiency of 83%, in good agreement with the value obtained from simulations (86%).

#252378 Received 21 Oct 2015; revised 26 Nov 2015; accepted 27 Nov 2015; published 14 Dec 2015

Figure 2(d) shows instead the light spectra measured on three different spots indicated by the markers in Fig. 2(b). The spectra show a clear separation, given that little overlap between curves measured at different spots is present, and are in good agreement with simulations (in dashed lines).

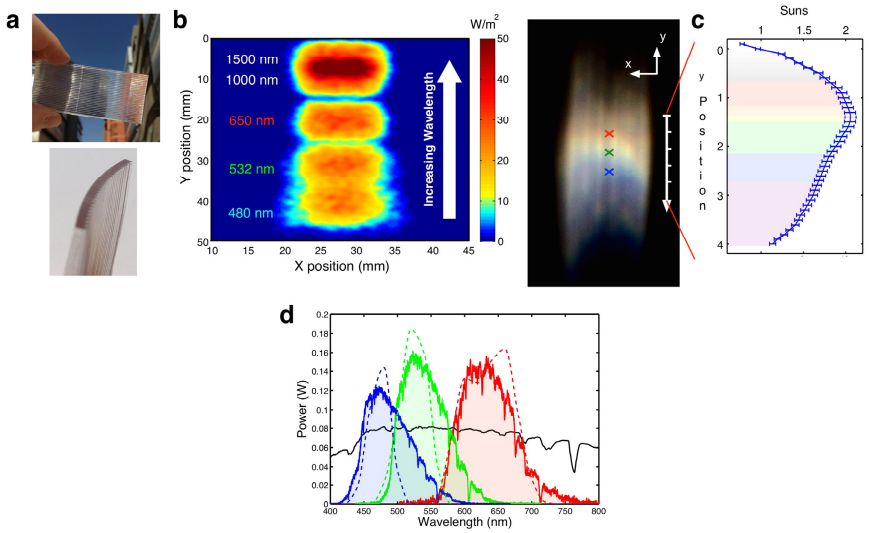

Fig. 2. (a) Pictures of the spectral splitter concentrator fabricated by injection molding, a low-cost technique used for commercial lenses. (b) Simulated two-dimensional map of the light intensity at the receiver surface for different wavelengths (480, 532, 650, 1000 and 1500 nm) together with a picture of the experimental light pattern obtained under solar light illumination. For the simulation, an intensity of 10 W/m^2 was set at the source. (c) Flux intensity under real sunlight measured over the profile of the light pattern, normalized to the measured on-site DNI of 62,8 mW/cm^2. (d) Spectra measured on three different spots, indicated in Fig. 2(b), along the y axis of the light pattern. Experimental results are compared with simulations (dashed lines). The black curve refers to the spectra of the direct sunlight.

2.2 Solar cells

To test the performance of the optical device, employing low-cost cells, we used a pair of CIGS solar cells. CIGS commands the second-largest market share among thin-film technologies after CdTe and have a module cost comparable with that of polyc-Si [14]. By varying the In/Ga ratio, its band gap can be tuned between, theoretically, ~1 eV for CIS (100% In) to 1.67 eV for CGS (100% Ga) [15]. This variation may be accomplished using several techniques [16–18] without significant process modification, although at the current stage wide band gap CIGS cells suffer from high recombination rates [19]. For this work, two CIGS devices with 30% and 50% Ga concentration were fabricated by pulsed electron deposition [20,21] and characterized to determine their spectral response and to quantify their power conversion efficiency (PCE) under full spectrum AM 1.5 illumination. The external quantum efficiencies (EQE) of the two cells, reported in Fig. 3(a), shows that the cut-off wavelength is approximately 1060 and 960 nm for the 30 and 50% Ga concentration cells respectively, corresponding to band gaps of 1.16 (referred to from here on as l-CIGS) and 1.3 eV (h-CIGS). While these values clearly are not optimized, the difference is sufficient to demonstrate in principle the performance of the splitter. In Fig. 3(b), current density versus voltage curves obtained under full spectrum illumination are shown for the two cells. It is noteworthy that contrary to what would be normally expected, the short circuit current density of the h-CIGS cell is higher than that of the l-CIGS. This can be explained by the lower EQE in the range 500-900 nm of the l-CIGS cell (see Fig. 3(a)). The parameters of the two devices,

#252378 Received 21 Oct 2015; revised 26 Nov 2015; accepted 27 Nov 2015; published 14 Dec 2015

which exhibit PCE values of 13.6% (h-CIGS) and 10.7% (l-CIGS) under 1 sun, are summarized in Table 1.

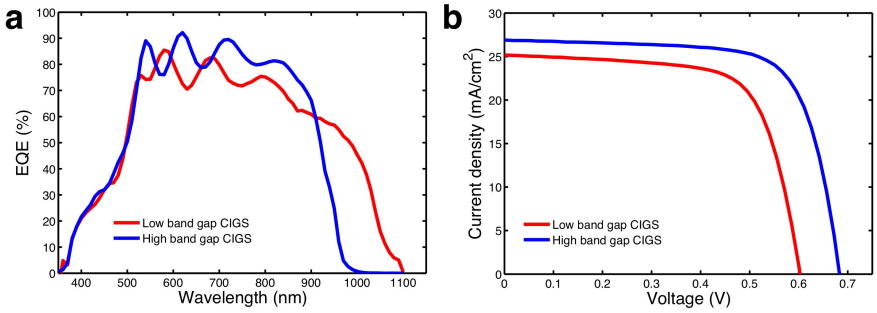

Fig. 3. (a) External quantum efficiency curves measured for the low and high band gap CIGS cells, having a band gap of 1.16 and 1.3 eV respectively. (b) Current density versus voltage curves of the two CIGS cells measured under full spectrum AM1.5 spectrum (100 mW/cm^2).

Table 1 Figures of merit of CIGS cells measured under AM 1.5 spectrum.

Parameters	J_{sc} (mA/cm^2)	V_{oc} (V)	F.F. (%)	PCE (%)
High band gap CIGS	26.8	0.685	74	13.6
Low band gap CIGS	25.15	0.608	70.1	10.7

2.3 Spectrum splitting concentrator system

To demonstrate the performance of the spectral splitter, we investigate the enhancement in PCE of the two cells (electrical power generated by the two devices over cell-incident optical power) when illuminated with the appropriate portion of the split light pattern projected by our splitter. The PCE of the two cells is equivalent to that of the spectral splitter photovoltaic system (optic + solar cells), if the splitter had an optical efficiency of 100%. While this represents an idealization, the optical efficiency of the splitter can be increased by covering the optics with an anti reflection coating, which in turn can also reduce PC degradation if designed as deep-UV reflector. We choose to illuminate the l-CIGS cell with wavelengths approximately from 850 to 1050 nm and the h-CIGS from 450 to 800 nm. The longer-wavelength part of the spectral range can be effectively captured with a single 0.4x0.4 cm^2 cell; the shorter wavelength portion is spread over a much larger distance due to the dispersion dependence of the splitting illustrated in Fig. 1(e), and therefore required several h-CIGS cells wired in parallel to capture the full range, effectively creating a single cell with dimension ~3x0.5 cm^2.

Figure 4(a) shows a schematic of the spectrum splitting concentrator system, where the splitter is positioned at a distance Z = 36 cm from the receiver, and the two cells previously described are placed adjacently on an x-y-z scanning stage at the receiver surface. The two cells are positioned in close proximity to each other and are aligned with the light pattern so that the h- and the l-CIGS cells are illuminated with high- and low-energy photons, respectively. Figure 4(b) shows the experimental spectral conversion efficiency (SCE) of the two cells together with the spectral content of the light illuminating them. The SCE measures the amount of energy converted by the solar cell as function of the wavelength of light and is given by [22] $SCE(\lambda)=\frac{q\lambda}{hc}\cdot EQE(\lambda)\cdot V_{oc}\cdot F.F.$, where V_{oc} and $F.F.$ are the open circuit voltage and the fill factor of the solar cells, respectively. The splitter concentrator was illuminated with outdoor sunlight having a measured direct normal insolation of 62.8 mW/cm^2. Figure 4(c) presents current and power density versus voltage curves of the two

#252378 Received 21 Oct 2015; revised 26 Nov 2015; accepted 27 Nov 2015; published 14 Dec 2015

CIGS cells measured independently in the configuration described in Fig. 4(a) (spectral splitter) and under full spectrum illumination (hereafter alluded as "reference"). It can observed that the spectral splitter concentrator increases the short-circuit current density of the high band gap cell by 150%, while the open-circuit voltage corresponding increase of 3.2%, which is less pronounced than expected probably due to non-uniform illumination [23]. The low band gap cell shows an increase in short-circuit current density and open-circuit voltage of 170% and 5% respectively. As a result, the power density of both cells is enhanced as illustrated in Fig. 3(c), where the measured peak power densities increased 155% and 182% for the h- and l-CIGS cell respectively. These large increases are the consequence of two factors: the narrower spectral profile of the light falling on the cell, and the high light intensity, which is increased by a factor of 1.5-2 over the investigated spectral range as shown in Fig. 2(c). To partially decouple these two effects we measure the light spectrum and total intensity over the whole cell area for both cells and recalculate the PCE of each cell as the ratio of the new output power density to the light flux intensity over the cell area. Table 2 reports the measured light intensity over the two devices and calculates their PCEs. We obtain a power conversion efficiency of the h-CIGS cell of 23±1% measured over the spectral range 450-850 nm and of 17.8%±1 for the l-CIGS cell calculated over 850-1050 nm range (referred to as 'efficiency over bandwidth' in Table 2). By weighting the power content of the two wavelength bands with respect to that of the full solar spectrum (53.55% and 14.55% respectively for the first and second band), we can sum these values to estimate a total system PCE over the full solar spectrum of 15.1±0.6, which means a maximum increase in efficiency of 15% with respect to the PCE of h-CIGS cell alone (13.6%). While the increase in efficiency is due to both concentration and splitting, the first contribution is expected to be smaller (around 25-30%). Therefore we can attribute most of the PCE enhancement to the splitting, which by minimizing hot carrier generation and thermalization enables more effective use of the incident light and additionally reduces the thermal load on the cells.

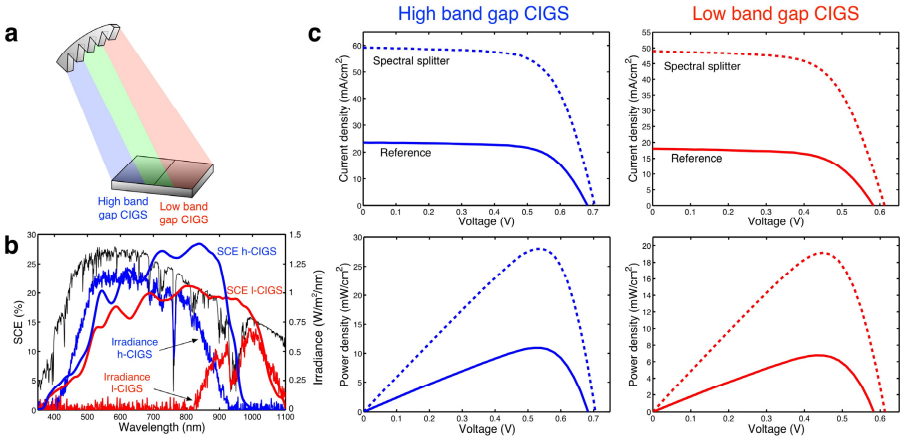

Fig. 4. (a) Schematic of the spectrum splitter concentrator system. The splitter concentrator is positioned at a distance of 36 cm from the receiver and the two cells are placed adjacently so that the high band gap cell is illuminated with high-energy photons and the low band gap cell with low energy-photons. (b) Experimental spectral conversion efficiency of the solar cells together with the spectra illuminating the two devices (blue for h-CIGS and red for l-CIGS). (c) Current and power density versus voltage curves of the two solar cells measured under full spectrum illumination (reference) and illuminated through the spectral splitter. Measurements were carried out under real sunlight illumination with a measured direct normal insolation of 62.8 mW/cm^2.

#252378 Received 21 Oct 2015; revised 26 Nov 2015; accepted 27 Nov 2015; published 14 Dec 2015

Table 2 Electrical and optical power density measurements over the two CIGS cells under spectrally splitted illumination.

	Peak output power density (mW/cm^2)	Optical intensity (mW/cm^2)	Efficiency over bandwidth (%)	Full spectrum PCE (%)
High band gap CIGS	28	122 ± 4	23 ± 1	12.6 ± 0.5
Low band gap CIGS	19.15	107 ± 3	17.8 ± 1	2.5 ± 0.1
			Total	15.1 ± 0.6

To further confirm our results, we computed the PCE of the two solar cells from the experimental SCEs and spectral irradiance curves reported in Fig. 4(b). From [22], we can write the PCE of the two devices as:

$$\eta_{two\_cells} = \frac{1}{P_{opt}^{h-CIGS}} \int E_{h-CIGS}(\lambda) \cdot SCE_{h-CIGS}(\lambda) d\lambda + \frac{1}{P_{opt}^{l-CIGS}} \int E_{l-CIGS}(\lambda) \cdot SCE_{l-CIGS}(\lambda) d\lambda \quad (3)$$

where $E(\lambda)$ is the spectral irradiance projected by the splitter and illuminating the two cells and P_{opt} is the corresponding optical power density. Figure 5(a) shows the spectral power converted by the two cells (blue for h-CIGS and red for l-CIGS). We obtain efficiencies of 12.45% and 2.29%, in excellent accordance with experimental results. To derive how much of an improvement the spectral splitter provided with respect to using a single type of PV cell, we calculate the Improvement over Best Bandgap (IoBB) [22], a metric defined as:

$$IoBB = \frac{\eta_{two\_cells}}{Max[\eta_{h-CIGS}, \eta_{l-CIGS}]} - 1 \quad (4)$$

where η_{h-CIGS} and η_{l-CIGS} are the full-spectrum efficiencies of the two CIGS cells. Summing the PCEs of the two cells illuminated through the splitter (12.45% and 2.29%) and taking the full-spectrum efficiency of the h-CIGS cell (13.6%), we obtain an IoBB of 8.38%. To evaluate the maximum potential of the configuration under analysis, we computed the PCE of the two cells illuminated with ideal spectral bands (i.e. no spectral components in the out-of-band regions). Figure 5(b) reports the spectral power converted in this case. We obtained a maximum combined PCE for the two cells of 15.37%, corresponding to an IoBB of 13%.

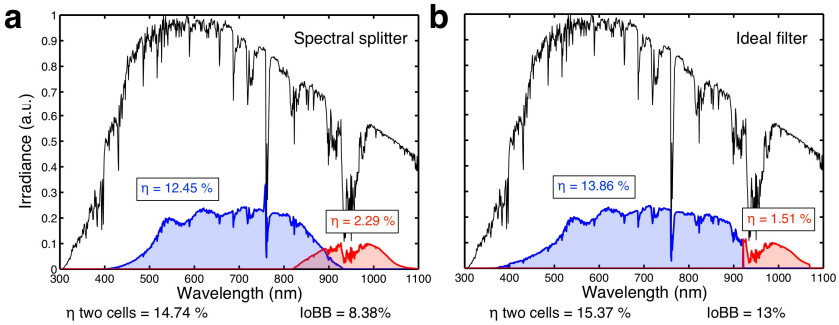

Fig. 5. SCE analysis of the two CIGS solar cells illuminated with our spectral splitter (a) and with an ideal filter (b).

As confirmed by the low values of IoBB, the band gaps of the cells used are clearly not optimized for maximum power conversion. In order to determine the collective efficiency of the spectrum splitting system (splitter + solar cells) implementing our optic with optimal

#252378 Received 21 Oct 2015; revised 26 Nov 2015; accepted 27 Nov 2015; published 14 Dec 2015

CIGS cells, a realistic analytical model was developed. Similarly to [22], we define the PCE of the spectrum splitting system η_{ss} (i.e. spectral splitter + N solar cells) as:

$$\eta_{ss} = \sum_{1}^{N} \eta_k^* = \sum_{1}^{N} \int T_k(\lambda) \cdot E_{AM1.5}(\lambda) \cdot SCE_k(\lambda) d\lambda \qquad (6)$$

where η_k^* is the filtered PCE of the kth cell and $T_k(\lambda)$ is the transmissivity of the splitter over the kth cell. For the calculation, we use the average value of the optical efficiency of the splitter $T_k(\lambda)$ = 0.86, assuming ideal filter selectivity (i.e. no out-of-band regions), and we implement the spectral conversion efficiency of state-of-the-art CIGS cells with different band gaps reported in Ref [16]. The graph in Fig. 6(a) shows that collective PCE values as high as 26.5% can be achieved when using 3 different band gaps, a 36% increase with respect to single junction CIGS cell (E_g = 1.16 eV, PCE = 19.4%). Although such increase is enough to justify the use of the splitter concentrator, further PCE enhancement could be achieved by improving the performance of high band gap CIGS cells, which at the current stage suffer from high recombination rates [19].

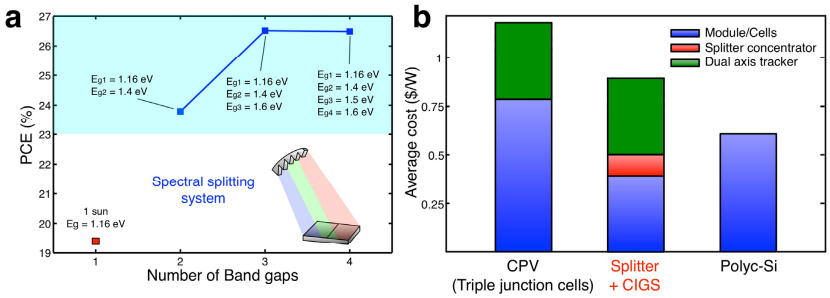

Fig. 6. (a) Power conversion efficiency of the spectral splitter concentrator system versus number of band gaps. The model used for the calculation accounts for the optical efficiency of the splitter and uses state of the art values of efficiency of CIGS cells. Band gap values are reported in the graph. The efficiency for 1 band gap is calculated without the splitter. (b) Average cost of PV technologies (CPV, splitter + CIGS and polyc-Si). Installation, electronics, operation & maintenance and other non-technology-specific related costs are assumed to be the same for the three photovoltaic options.

3. Cost evaluation

To qualitatively evaluate the economic impact of our splitter – CIGS cells system, we compare the cost (in $/W) against the alternative technology, i.e. concentrating photovoltaics (CPV), and against plain poly-Si photovoltaic modules, which represent the standard in the PV market. To simplify the comparison, exemplified in Fig. 6(b), we will limit our analysis to the cost of the module and, when required, to that of optic and mechanical tracker. Installation, electronics, operation & maintenance and other non-technology-specific related costs are not accounted for. For a list of the requirements of each technology see Table 3.

Table 3 Requirements, efficiency and costs of photovoltaic conversion systems.

Technology	CPV	polyc-Si	Spec. Splitter - CIGS
Requirements	- MJ PV cells (m) - concentrator (c) - double axis solar tracker (2Dt)	- polyc-Si module	- CIGS module (m) - spectral splitter (s) - double axis solar tracker (2Dt)
Efficiency (commercial modules)	35.9 ± 1.8%[26]	18.5 ± 0.4%[26]	26.5%
Cost ($/W)	m + c: 0.77 2Dt: 0.45	0.47 - 0.78	m: 0.26 – 0.5 s: 0.1 2Dt: 0.45
TOTAL COST ($/W)	1.22	0.47 - 0.78	0.81 – 1.05

#252378 Received 21 Oct 2015; revised 26 Nov 2015; accepted 27 Nov 2015; published 14 Dec 2015

CPV technology uses high concentration optics, efficient MJ modules and double axis solar trackers. Although MJ solar cells have demonstrated much higher efficiencies compared to plane c-Si modules under one sun illumination [3], their cost is two orders of magnitude greater than that of the leading product in the market [24]. For this reason, MJ solar cells are combined with high concentration optics (~500x) that allow to reduce the costs by producing more energy out of the same area. The estimated minimum cost of a CPV module (including lenses) is 0.77 $/W [24], indicated in blue in Fig. 6(b). The use of high concentration mandates the use of highly stable double axis trackers, as high-concentration systems have an inherently very narrow optical acceptance cone. The high cost of such tracking systems (around 0.45 $/W [25], indicated in green) prices these systems out of the market for terrestrial applications, unless very specific high DNI irradiance conditions exist.

In contrast, our proposed spectral splitting system may achieve cost reduction in both the PV and the tracking, with similarly low cost in the optics. The price of the splitter, including material, production and tooling, is as low as 0.1 $/W assuming production of ~1 million pieces, which has a small impact on the overall cost of the system (the cost was derived using the injection molding cost estimator at the following website http://www.custompartnet.com/estimate/injection-molding/). On the absorber side, we use the cost of CIGS plain modules (0.47 – 0.79 $/W [14]) as starting reference, given that the increase in cost deriving from the lateral band gap grading of the proposed new modules is marginal. Our spectral splitter + CIGS system allows for increased collective PCE compared to plain CIGS modules (average efficiency 15% [26]) as a result of the splitting/concentration and given the small dimension of the cells, which generally exhibit better performance than large area modules. By scaling down the cost of the PV system according to the increase in efficiency (from 15 to 26.5% for a three-band-gap system), we obtain a cost in the range 0.26-0.50 $/W. In terms of mechanical system, our solution still demands a two-dimensional tracker, but the requirements are less stringent compared to CPV systems. While precise tracking is required along the direction of the light spreading (y-axis), with a simulated acceptance angle of 0.24 degrees, a less accurate alignment along the x-axis is sufficient to allow for the proper operation of the system given the low concentration factor of the optical device along this direction (acceptance angle of 0.6 degrees). Compared to low-cost Fresnel lenses for CPV systems, which typically exhibit off-axis tolerance angles below 0.25 degrees [27], our design enables reduction of the mechanical tracker precision requirements.

In summary, the cost comparison in Fig. 6(b) shows that the splitter + CIGS system provides a competitive alternative to CPV for broadband solar conversion. The price of our system is also surprisingly reasonable in comparison to the most widely adopted PV modules, polyc-Si, which are generally exploited without the need for concentration or solar tracking at a cost of 0.47 – 0.78 $/W [14] and an average commercial efficiency of 18% [28]. Moreover, the cost of our system can be further reduced by increasing its PCE with the integration of wide-band low-cost highly performing PV solar cell technologies (i.e. CdTe or Perovskites). These results allow us to conclude that by optimizing fabrication practices and the design of the cells, our system has the potential to compete with polyc-Si technology in terms of energy production costs.

4. Conclusions

In summary, in this work we have proposed a novel paradigm for spectral splitting that is the result of a holistic approach aimed at lowering the cost of PV technology. Both components of the system (optical element and PV) are designed to maximize their performance while keeping their costs low. The optical element, designed to fulfill the requirements of industrial production, is an inexpensive plastic lens capable of concentrating the sunlight while allowing for its continuous spectral separation. The spectrum obtained as output of the splitter is fed into inexpensive, band-gap matched thin-film CIGS cells, leading to an increase in PCE of 15%, with efficiencies as high as 26.5% achievable with a three-band-gap system. Although

#252378 Received 21 Oct 2015; revised 26 Nov 2015; accepted 27 Nov 2015; published 14 Dec 2015

these numbers are lower compared to the efficiency of CPV, we have shown that our approach can provide a more cost-effective pathway for broadband light-to-electricity conversion. The concept presented here shows that economically competitive PV modules can be developed by combining current commercial solutions into innovative designs.

Acknowledgments

We would like to thank Mrs. Yamila Omar for proofreading the manuscript and for fruitful discussions. We would like also to thank Dr. Tim Milakovich and Prof. Eugene A. Fitzgerald from the Massachusetts Institute of Technology for their support in the early stage of the project.

#252378 Received 21 Oct 2015; revised 26 Nov 2015; accepted 27 Nov 2015; published 14 Dec 2015